Omnidirectional planar Antennas for PCS-Band Applications using Fiberglass Substrates.

Humberto Lobato-Morales[1], Alonso Corona-Chavez[2], L. Gerardo Guerrero-Ojeda[1].

1. *Universidad de las Américas-Puebla.*
Sta. Catarina Mártir. Cholula, Puebla. 72820. México.
2. *National Institute for Astrophysics, Optics and Electronics.*
Luís Enrique Erro No. 1, Tonantzintla, Puebla. 72000. México.
humberto.lobatoms@udlap.mx

Abstract

The design, construction and characterization of planar antennas implemented using fiberglass substrate is presented. For PCS-band frequencies (1.9 GHz), planar antennas are usually constructed of copper films on low-permittivity low loss substrates such as Duroid. Duroid improves the antenna efficiency due to its uniform structure for microwave designs, but its main disadvantage is its high cost. Good antenna performance can be achieved using other substrates, like fiberglass, that is one of the most common materials to construct DC printed circuit boards. Dipoles, patches and collinear arrays are implemented using fiberglass substrates achieving good performance over PCS band. A directional wideband Vivaldi antenna is designed and implemented using the same fiberglass substrate for gain measurements.

Index terms *– dipole, patch antenna, OMA antenna, Tripatch antenna, Vivaldi antenna.*

1. Introduction

A very important task of mobile communications is the antenna behavior. Its radiation characteristics are much related with the structure and size of resonators, and substrate thickness and dielectric constant (ε_r). Omnidirectional arrays are usually used in micro and pico-cell base-stations due to the small covered area, and because of the high user's traffic and low transmitted power, high gains must be achieved.

The growth of radiating and resonating planar structures has introduced a level of miniaturization and performance improvement of RF/microwave devices. Patch antennas have been used in many applications in the last ten years due to its planar structure, small size and radiation characteristics. Many substrates have been employed to support the thin film resonators. Low-permittivity, low loss-substrates such as *Duroid* improve the antenna efficiency due to its uniform structure for microwave designs, but their main disadvantage is its high cost. Fiberglass is the most used material for *DC* electronic implementations, like printed circuit boards. Fiberglass layers covered by copper films are commercially available, and planar resonators can be constructed using printed circuit technology. Fiberglass structure is not as uniform as Duroid in terms of manufacturing processes [1]. There exist little air bubbles distributed among the body and non uniformity of thickness [1], but at PCS frequencies (1.9 GHz) the disadvantage is overcome due to the higher size wavelengths. With higher frequency devices, more uniformity materials must be chosen in order to minimize imperfection dimensions respect to the wavelengths used. At lower frequencies (f_c<500 MHz) resonating structures present high dimensions making planar antennas not to be an optimum choice. Instead loop and helicoidal antennas are implemented [2]. The proposed antennas are implemented using fiberglass substrates covered by copper films over both sides. The antennas are coupled to 50 Ω standard impedance [2]. A fiberglass substrate characterization is realized in order to obtain its permittivity coefficient ε_r [1].

The rest of the paper is organized as follows. Section 2 presents the fiberglass substrate characterization; section 3 describes the design and construction of the proposed antennas; characterization of the antennas is reported in section 4; and conclusions are presented in section 5.

2. Fiberglass substrate characterization

In order to obtain the permittivity coefficient ε_r of the fiberglass substrate, a single λ_g/2-lenght resonator is implemented according to

$$\lambda_g = \frac{c}{f_c\sqrt{\varepsilon_r}}, \qquad (1)$$

where λ_g is the guided wavelength, c is the speed of light and f_c represents the resonant frequency. It is assumed that the value of ε_r is located between 3 and 7, so it is started with a proposed value of 5. The structure of the resonator is shown in figure 1.

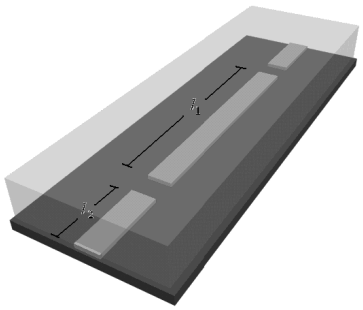

Figure 1. λ_g/2-lenght resonator.

0-7695-3120-2/08 $25.00 © 2008 IEEE
DOI 10.1109/CONIELECOMP.2008.6

IEEE computer society

The resonator is implemented for a 1.3 GHz resonance, so its dimensions are l_1=51 mm, l_2=6 mm, with 1 mm gaps in order to achieve a weakly electric coupling; the width of the lines is of 2.8 mm. The substrate thickness is of h=1.6 mm. The insertion losses S_{21} obtained from the network analyzer shows the main resonance at 1.584 GHz. Simulations of this structure are realized with same dimensions and only varying ε_r in order to adjust the real value. Table 1 shows three simulated frequency resonances for different values of ε_r.

ε_r	f_r
3	1.89
7	1.3
4.4	1.59

Table 1. Resonances and its ε_r.

From simulations, it is concluded that a value of 4.4 for ε_r is of good agreement with measured S_{21} curve and resonance. Also a 1.9 GHz resonator is implemented in order to corroborate this data, obtaining the desired results.

3. Design of the antennas

A planar dipole antenna, two rectangular patch antennas, and two arrays of patch antennas are designed and implemented at PCS band frequencies.

Dipole antennas are the oldest and simplest antenna type ever used [2] [3]. The simplest dipole consists of a couple of rods in opposite directions. Dipoles present an omnidirectional radiation pattern that is desired for mentioned wireless applications [4]. Figure 2 shows an omnidirectional radiation pattern produced by a $\lambda/2$ length dipole [3]. The designed and implemented planar dipole consists of a $\lambda/2$ thin line strip that is coupled to a transmission line section in the same substrate.

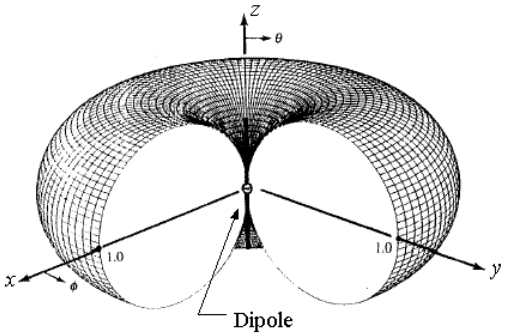

Figure 2. Omnidirectional radiation pattern of a dipole.

The dipole length can be obtained from the input resistance [3]

$$R_{in} = 24.7G^{2.5}. \quad (2)$$

The desired input impedance is 50 Ω, so substituting it in (2) and making $G=l\pi/\lambda$, where l is the dipole length, we obtain

$$l = 0.422\lambda. \quad (3)$$

The central operation frequency is 1.9 GHz so the correspondent wavelength in free space is λ=157.9 mm. The overall strip dipole length results l=66.6 mm.

The strip width is of ≈5 % of its length. A transmission line is implemented over the substrate in order to conduct the signal to the dipole and avoid radiation out of it. The ground plane of the transmission line is of 10 times the width of the line.

Based on simulations the feed point of the dipole is moved from the center and the dipole length is lightly increased in order to improve the input impedance. The final design is shown in figure 3 with its correspondent dimensions.

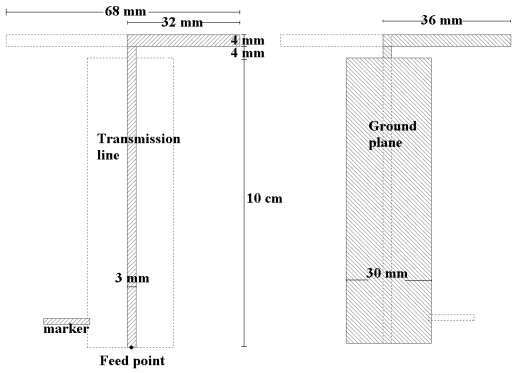

Figure 3. Dipole antenna.

The design of patch antennas is mainly based on *transmission line model* [5] and *cavity model* [3]. From the first one, the effective permittivity, which forms the combination of the substrate and air permittivity, is

$$\varepsilon_{reff} = \frac{\varepsilon_r + 1}{2} + \frac{\varepsilon_r - 1}{2}\left[1 + 12\frac{h}{W}\right]^{-\frac{1}{2}}, \quad (4)$$

where h is the substrate thickness and W is the width of the resonator. For the TM_{010} dominant mode the resonator length L can be approximated as

$$L \approx \frac{1}{2f_0\sqrt{\varepsilon_{reff}}\sqrt{\mu_0\varepsilon_0}}, \quad (5)$$

where f_r is the operation frequency, μ_0 and ε_0 are the substrate permittivity and permeability coefficients. A good approximation for the patch width W is

$$W \approx \frac{v_0}{2f_r}\sqrt{\frac{2}{\varepsilon_r + 1}}. \quad (6)$$

The variable v_0 represents the speed of light in free space. The size of the patches are L=37 mm by W=22 mm. The feed line is placed orthogonal to L in order to achieve the desired 50 Ω impedance by moving it a distance y_0 along L in the simulations. A way to obtain y_0 is from the input resistance function which shows the input resistance as a function of the normalized y_0 [3]. This plot is shown in figure 4.

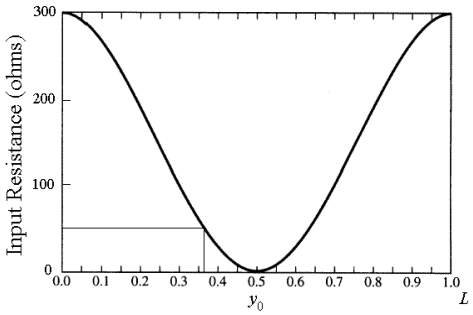

Figure 4. Normalized y_0.

According to simulations, the resonator dimensions are adjusted and the final dimensions are L=38 mm, W=26 mm and y_0=14 mm. The feed line width is of 4 mm. The overall substrate dimensions are 73×57 mm and the resonator is located at the center. Figure 5 shows the rectangular patch resonator.

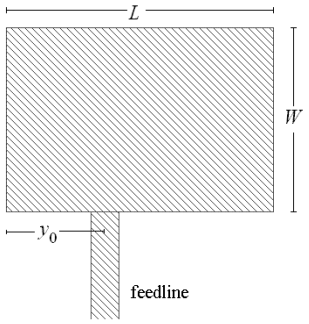

Figure 5. Rectangular patch resonator.

An improvement in radiation behavior can be achieved by placing two small slots in the resonator at each side of the feed line [3]. A second rectangular patch antenna is designed with these slots. Patch dimensions are the same of the first antenna. Deep of slots are generated based on simulations, and results of 3 mm and a width of 4 mm each one. The final design of the patch with the slots is shown in figure 6.

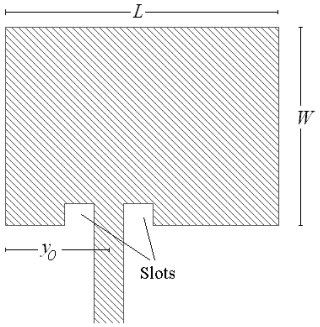

Figure 6. Patch resonator with slots.

An antenna with three patch resonators is designed in order to increase the bandwidth [6]. The resonant frequencies for each of the patches are 1.85, 1.9 and 1.99 GHz which correspond to lower, central and upper PCS band frequencies [13]. Patch dimensions are calculated using (5) and (6). This antenna is fed at the central patch in coaxial mode with an SMA type connector. The length L_3 starts from the feed point. Antenna structure is shown in figure 7.

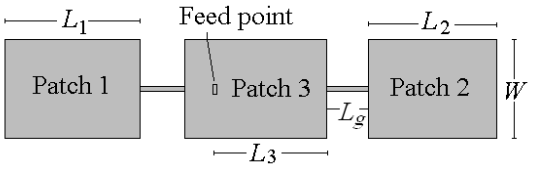

Figure 7. Tripatch antenna.

The final dimensions adjusted from the simulations are L_1=40 mm, L_2=38 mm, L_3=35 mm, W=26 mm. The overall length of patch 3 is of 42 mm, but the effective resonance section is L_3. Distances between the patches (L_g) are of 13 mm length. Tripatch antenna presents a non pure omnidirectional radiation pattern due to the constructive/destructive signal phases generated between neighbor patches.

OMA (Omnidirectional Microstrip Array) antennas are widely used for Wi-Fi applications [7]. An OMA antenna consists of alternated and aligned transmission line segments. Gains of about 5 dBi [8] can be achieved with this type of antenna array. A seven segment OMA antenna is shown in figure 8.

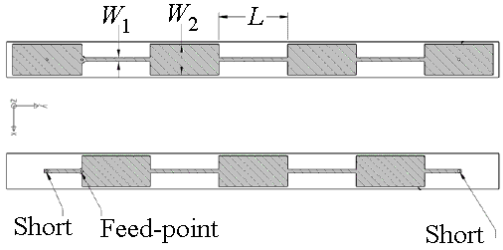

Figure 8. Seven segment OMA antenna.

The length of the segments are $L=\lambda_c/2$ where λ_c is the wavelength in the substrate [7]. W_1 and W_2 are adjusted to form a 50 Ω transmission line in each of the segments [8]. Approximated dimensions correspond to $W_2 \approx 5W_1$, but these values vary due to the substrate thickness and permittivity. W_1 is about 5 % of L. The feed point is located at the transition of the first and second segments. The external segments are shorted to its correspondent ground planes at the center of them.

Based on simulations and adjustments, the final dimensions are L=37 mm, W_1=2 mm and W_2=16 mm. This antenna is fed using an SMA connector In order to realize the measurements it is necessary a wideband antenna to calculate gains. Vivaldi antennas are commonly designed to operate at maximum frequencies of 5 to 30GHz [9], [10] and [11].

The antenna is fed using a parallel conductor transmission line that ends in an aperture. Figure 9 shows the structure of a Vivaldi antenna.

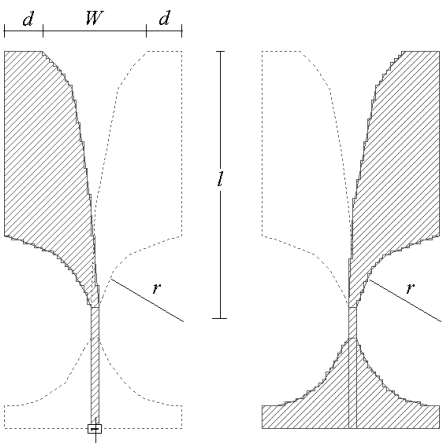

Figure 9. Structure of a Vivaldi antenna.

The aperture follows an exponential trajectory for each side of the substrate, and ends in a width *W*. The transition from the ground plane to the aperture is *r*. The aperture geometry is determined by [10]

$$y = c_1 e^{Rs} + c_2, \tag{7}$$

where

$$c_1 = \frac{x_2 - x_1}{e^{Rz_2} - e^{Rz_1}}, \tag{8.a}$$

$$c_2 = \frac{x_1 e^{Rz_2} - x_2 e^{Rz_1}}{e^{Rz_2} - e^{Rz_1}}. \tag{8.b}$$

The variables (x_1, z_1) and (x_2, z_2) are the initial and final coordinate points of the aperture. *R* is a variable that shifts the aperture ratio. The antenna behavior is mainly dependent of *R* [10]. For a good performance *l* must be greater than λ_0 and $W \approx \lambda_0/2$, where λ_0 is the central operation frequency.

The described Vivaldi antenna presents an approximated bandwidth from 1.5 to 8.5 GHz. The final dimensions are *r*=45 mm, *l*=140 mm, *W*=54 mm and *d*=20 mm.

All the antennas are fed by using SMA type connectors [12].

4. SIMULATION AND EXPERIMENTAL RESULTS

All the simulations are carried out using [14]. Figure 10 shows the return loss (simulated and experimental) of the dipole antenna. It has a bandwidth of 26 % for S_{11}<-10 dB.

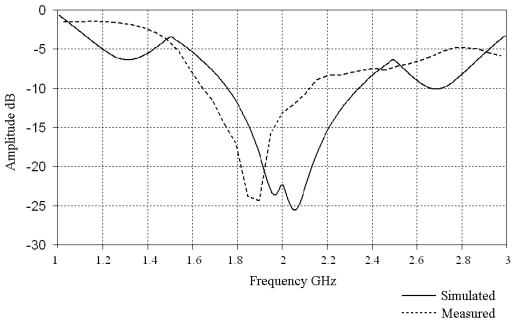

Figure 10. Dipole antenna return loss.

The return losses of the two designed rectangular patch antennas are plotted in figure 11.

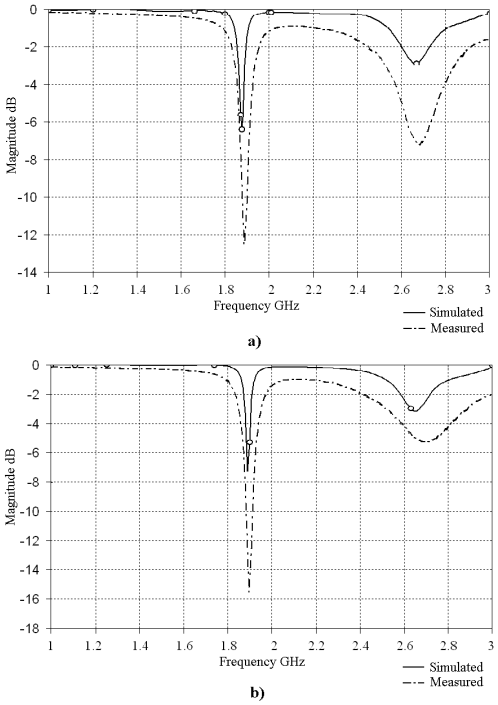

Figure 11. Return losses, a) Patch antenna, b) Slotted patch antenna.

It is noticeable that the bandwidth is narrower compared to that of the dipole, so patch antennas are more band selective. Also the slots at both sides of the feed line improve the performance of the rectangular patch resonator.

The return loss peak of the first patch antenna is located at -12 dB while the slotted patch antenna generates its peak near -16 dB. The correspondent bandwidths are 1.18 % and 1.54 % respectively for S_{11}<-10 dB.

The tripatch antenna generates a return loss S_{11} curve which is plotted in figure 12.

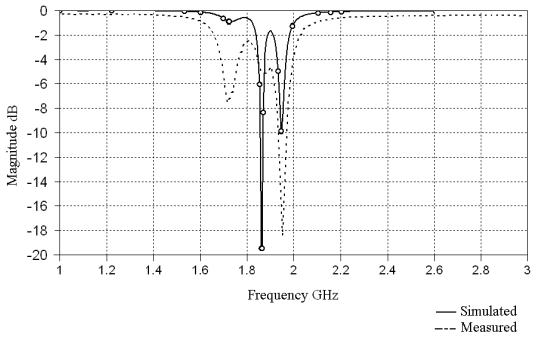

Figure 12. Tripatch antenna return loss.

From figure 12 the three resonances can be distinguished at 1.75 GHz, 1.85 GHz and 1.95 GHz. Differences between the simulated and measured curves are due to manufacturing tolerances. The bandwidth for this antenna results of 1.88 %.

The OMA antenna generates a return loss curve which is plotted in figure 13.

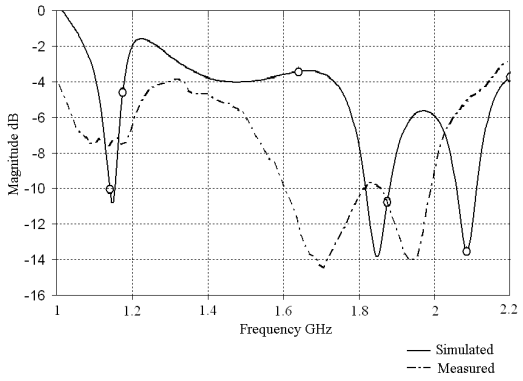

Figure 13. OMA return losses.

It is shown that wider bandwidth is obtained, compared to the dipole and rectangular patch antennas. The measured bandwidth is 19 % for S_{11}<-10dB.

The measured return loss curve of the wideband Vivaldi antenna is shown in figure 14.

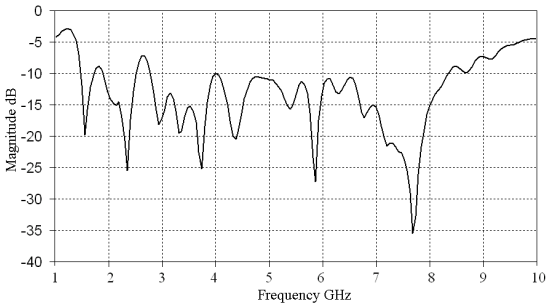

Figure 14. Vivaldi antenna return losses.

For this Vivaldi antenna the bandwidth results of 5:1, for a return loss smaller than -10 dB.

To measure the gain of the antennas the experimental setup shown in figure 15 is implemented. To set the reference a dipole was measured first. All the measurements are performed in co-polarization at their center frequency and only the *E* plane was measured.

Figure 15. Antenna gain measurement.

Table 2 shows the gain values for each of the antennas.

Antenna	Gain (dBi)
Dipole	2.15
Patch antenna	2.15
Slotted patch antenna	2.15
Tripatch antenna	4.15
OMA antenna	7.15
Vivaldi antenna	9.15

Table 2. Antenna gain.

It is noticeable that the maximum gain for an omnidirectional radiation pattern is achieved by the OMA antenna due to the number of segments. The patch antennas present the same gain as the dipole because they present only one resonating structure.

Directive antennas generate higher gains due to the energy concentration in the main lobe. It is the case for the wideband Vivaldi antenna, which performs a gain of 9.15 dBi at a frequency of 1.9 GHz.

5. CONCLUSIONS

Six antennas were successfully implemented using a low cost fiber glass substrate. All the antennas were built and tested with good agreement between experimental and simulated results. The largest gain at the center frequency was obtained with the wideband Vivaldi antenna, however, the highest gain for the omnidirectional antennas was given by the 7-segment OMA antenna. Also lower resonator dimensions were accomplished due to the higher fiberglass dielectric permittivity compared to that of a common Duroid substrate.

6. REFERENCES

[1] Alonso Corona-Chavez, *Characterization of fiberglass substrate*, Technical report, INAOE, July 2005.

[2] Simon R. Saunders, "*Antennas and Propagation for Wireless Communication Systems*", John Wiley and Sons, West Sussex, England 1999.

[3] Constantine A. Balanis, "*Antenna Theory: Analysis and Design*", John Wiley and Sons, second edition, 1997.

[4] Wayne Tomasi, "*Sistemas de Comunicaciones Electrónicas*", Prentice Hall, cuarta edición, México, 2003.

[5] David M. Pozar, "*Microwave Engineering*", John Wiley and Sons, second edition, 1998.

[6] Sonnet Software, *Sonnet® User's Manuals*, Application Examples, Antennas, Tripat, Sonnet ® Release 10 – Version 10.51 Lite.

[7] Bancroft, Randy; Bateman, Blaine, *Design of a Planar Omnidirectional Antenna for Wireless Applications*, Centurion Wireless Technologies Westminster, Colorado.

[8] Bancroft, Randy; Bateman, Blaine, *An Omnidirectional Planar Microstrip Antenna*, IEEE Transactions on Antennas and Propagation, Vol. 52 No. 11, November 2004.

[9] Computer Simulation Technology, *Vivaldi antenna*, Found on April 2006, Last modified: 9/6/2005, Technical report, URL: http://www.cst.com/Content/Articles/article15.aspx

[10] Kim Sang-Gyu, Kai Chang, *Ultra Wide Band Exponentially – Tapered Antipodal Vivaldi Antenna*, Department of Electrical Engineering, Texas A&M University.

[11] Adrian Sutinjo, Edwin Tung, *The Design of a Dual Polarized Vivaldi Array*, Murandi Communications Ltd., Calgary, Canada.

[12] Johnson Components, *RF Connector Application Guide*, Cambridge Products.

[13] L. Gerardo Guerrero-Ojeda, *Tópicos Avanzados de Comunicaciones*, course notes, Universidad de las Américas – Puebla, Primavera 2005.

[14] Sonnet Software, *Sonnet®*, Release 10 - Version 10.51 Lite.